2

CONF-9004466--74

SOL-GEL FILM FORMATION BY DIP COATING

SAND--90-0146C

DE90 015167

ALAN J. HURD and C. JEFFREY BRINKER
Sandia National Laboratories, Albuquerque, NM 87185-5800

INTRODUCTION

Manufactured coatings are fundamental to our Information Age Society. From Wall Street to the local library, much of the world's production of new wealth and wisdom is necessarily archived on magnetic, optical, or photographic coatings. Expanding markets can be expected for coatings on optics, integrated circuits, microsensors (including bioactive layers), and separation membranes. To track the demand of these and other future applications, the materials and processing of coatings deserve exploration.

Sol-gel films, belonging to the broad class of coatings applied via a liquid carrier, have enjoyed recent attention. Although they have been studied since WWII [1], their use has not been widespread in spite of potential advantages, not the least of which is simplicity. Whereas deposition from the gas phase requires expensive vacuum equipment, sol-gel coatings can usually be applied with a minimum of investment while often surpassing the conventional coating in quality.

Deposition by dip coating proceeds through overlapping stages: When a substrate is withdrawn slowly from a sol, containing polymeric or colloidal species in suspension, a film of liquid becomes entrained on the surface. The film thins through gravitational draining, capillary-driven flows, and, most importantly, evaporation, culminating in a well defined drying line beyond which lies a nearly dry film. When the recession speed of the drying line (relative to the substrate) matches the withdrawal rate, steady state conditions (relative to the reservoir) prevail.

In the meantime, the particles in the entrained liquid, which are often reactive and tend to gel, experience a rapidly concentrating environment. Whereas the dilute sol in the reservoir might gel in months, the entrained sol has only seconds to react, albeit in less dilute states. The sol may pass through a transient gel-like state before the drying line passes; during the final stage of evaporation, large capillary stresses can develop in the network, causing it to collapse partially. The remnant porosity is evidence for the fleeting "gel" state, and varying its structure through chemical and physical means serves to tune the film characteristics. Thus sol-gel thin films can differ greatly in structure from bulk xerogels or aerogels [2] if desired.

Indeed, it is this structural diversity that makes sol-gel films interesting from an application standpoint, not to mention the advantages of low temperature processing at ambient pressure.

In this paper, the physical aspects of sol-gel film formation are discussed. The equations governing the steady state film profile, controlled by hydrodynamic flow, capillary pressure and evaporation, are presented along with representative data obtained by imaging ellipsometry [3]. Some issues concerning capillary collapse are also addressed.

THE DRAG OUT PROBLEM

The hydrodynamic factors in dip coating were first calculated correctly by Landau and Levich [4] and recently generalized by Wilson [5]. These authors did not consider the case of evaporation. A first attempt at such a theory was made by Hurd and Brinker [6], who assumed that the evaporation rate was constant along the entrained liquid film and ignored surface tension. The predicted thickness profile was a linear wedge, connecting to the reservoir with a ~100 Å radius of curvature.

The profile data for ethanol in Fig. 1a clearly indicaue that the evaporation rate is not constant, but accelerates near the drying line, as manifest by the more rapid thinning there. In the following development, the local evaporation rate is shown to be controlled by the vapor diffusion away from the film; near the drying line the evaporation rate increases in singular fashion and this singularity is manifested in the thickness profile. An interesting feature of this phenomenon is the fact that the strength of the singularity is geometry dependent: The effect of changing the substrate from a plane to a line (cylinder with small radius) changes the profile in a characteristic way.

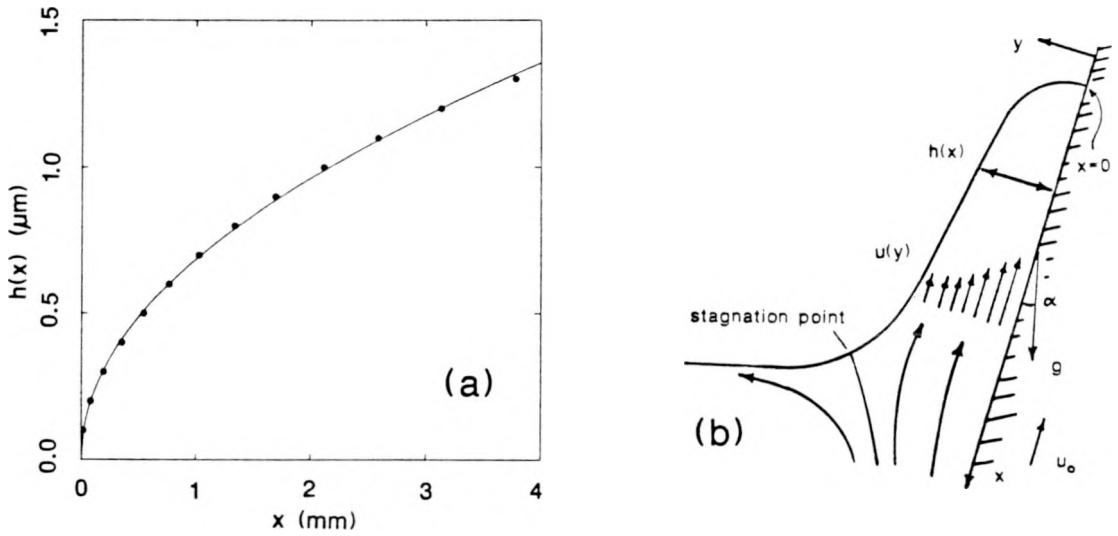

Figure 1. (a) Thickness profile for ethanol (note the expanded thickness scale). The fit represents $h(x) \sim x^{\eta}$ with $\eta=1/2$. (b) Geometry.

In view of the thinness of the film compared to its width and breadth and small slope of the entrained layer (Fig. 1), a lubrication approximation applies, in which flow is parallel to the substrate and only gradients normal to the substrate are important, i.e. $\vec{u}\cdot\nabla\vec{u}\simeq 0$. In the region of the reservoir meniscus, the liquid cannot be considered thin, but there the flows are negligible. Thus we expect the profile of a static gravitational meniscus to apply at the bottom (where evaporation effects are not important). Here we set up the full problem for later reference, embellishing Wilson, although we discuss only the thin film in the region for which we have optical profiles--not too close to either the drying line or the meniscus.

The substrate is pulled from the reservoir at an angle α from the vertical. (This geometry removes infinite derivatives in the development. It is permissible, of course, to take the limit $\alpha\to 0$ in the end.) Let x measure distance along the substrate from the drying line toward the reservoir, and let y be normal to the film (Fig. 1b). The Navier-Stokes equations in the lubrication approximation are

$$0 = -\frac{\partial p}{\partial x} + \eta \frac{d^2 u}{dy^2} + \rho g \cos\alpha \quad , \tag{1}$$

$$0 = -\frac{\partial p}{\partial y} - \rho g \sin\alpha + \frac{d\Pi(y)}{dy} \quad , \tag{2}$$

where η is the viscosity, ρ is the liquid density, $\Pi(y)$ is the disjoining pressure, u is the flow in the x direction, and p is the total pressure. The boundary conditions are

$$u = -u_0 \qquad \text{on } y = 0 \quad , \tag{3}$$

$$\frac{du}{dy} = 0 \; ; \; p = -\gamma\kappa \qquad \text{on } y = h(x) \quad , \tag{4}$$

where γ is the surface tension coefficient, κ is the curvature and h(x) is the profile of the liquid. The curvature is given by the formula

$$\kappa = \frac{d^2h/dx^2}{\left(1 + (dh/dx)^2 \right)^{3/2}} \quad , \tag{5}$$

and by integrating Eq. (2) with its boundary condition the pressure can be found. Next, the velocity can be found from Eq. (1) to be

$$u = -u_0\left[1 + f(x)h(x)y - \frac{1}{2} f(x)y^2 \right] \quad , \tag{6}$$

where $f(x)=(\rho g/\eta u_o)(\sin\alpha\, h_x-\cos\alpha)-(\gamma/\eta u_o)\kappa_x-(1/\eta u_o)(d\Pi(h)/dh)h_x$. An equation for the steady state h(x) can be found by equating the mass flux $J(x)=\int_0^h \rho u\, dy$ to the evaporative loss between x and the drying line,

$$J(x) = -\int_0^x E(x)\, dx \quad . \tag{7}$$

The quantity E(x) is the evaporation rate (g cm^{-2} sec^{-1}) at point x.

Let $d=(\eta u_o/\rho g)^{1/2} \approx 10$ μm, $D=(\gamma/\rho g)^{1/2} \approx 1$ mm (the gravitational capillary length), $Ca=\eta u_o/\gamma \approx 10^{-5}$ (the capillary number), and $\delta=(Ca)^{1/6}$. Following Wilson, we scale h by δd and x by $d^{1/3}D^{2/3}$ yielding

$$\phi^3 \frac{d}{d\xi} \frac{\phi_{\xi\xi}}{(1+\delta^4\phi_\xi^2)^{3/2}} = 3[\phi - j(\xi)] - \pi_\xi\phi^3\phi_\xi - \delta^2\cos\alpha\, \phi^3 + \delta^4\sin\alpha\, \phi^3\phi_\xi . \tag{8}$$

Here $\phi=h/(\delta d)$, $\xi=x/(\delta L)$, $j(\xi)=(\delta d\rho u_o)^{-1}\int_0^x E(x)dx$, and $\pi(\xi)=\Pi(h)/(\delta L\gamma)$. The disjoining pressure Π can include van der Waals, osmotic, and double layer forces. We limit ourselves to regimes in which Π is neglible.

Now we focus on the thin entrained film within, say, several microns of the drying line (where the profile slope ϕ_ξ is still small). Equation (8) shows that near the drying line for small ϕ

$$\phi \to j(\xi) \qquad (\xi \to 0) \quad . \tag{9}$$

The local evaporation rate E(x) must be equal to the diffusive flux of vapor, $-D_v(\partial c/\partial y)_{y=h}$, from the liquid surface. D_v is the vapor diffusivity and c is the vapor concentration. The vapor concentration follows the steady state diffusion equation,

$$\nabla^2 c = 0 \quad ; \quad c = c_o \text{ on the liquid surface} \quad , \tag{10}$$

$$c_y = 0 \quad \text{on the dry substrate } x < 0 \quad , \tag{11}$$

where the first boundary condition, borrowed from Maxwell's study of evaporating drops [7], applies when the mean free path of the vapor molecules ($\sim 10^3$ Å) is small compared to the extent of the liquid surface. The second boundary condition ensures there's no evaporative source above

the drying line; it can be trivially satisfied by symmetry after reflecting the problem near the drying line about the plane y=0.

Equation (10) is equivalent to that for the electrostatic potential around a conductive object, with the electric field at the surface being analogous to the evaporation rate E(x) and the flux $j(\xi)$ analogous to the charge accumulation between 0 and ξ. Near any sharp boundaries, the electric field (evaporation rate) diverges but the charge (vaporized mass) must remain integrable. This divergence in evaporation accounts for the blunt profile noted in Fig. 1 as shown below.

Since the profile h(x) is not known a priori, Eq. (10) is a free boundary problem. However, since the entrained film is very thin compared to its breadth and length, the vapor sees it as infinitely thin; hence, its detailed shape doesn't matter. The solution for the potential and field near the edge of a thin sheet is [8]

$$c \approx c_o - a_1 r^{1/2} \sin(\theta/2) \quad , \tag{12}$$

$$E = - D_v \frac{\partial c}{\partial y}\Big|_{y=0} \approx D_v a_1 x^{-1/2} \quad , \tag{13}$$

where (r,θ) are cylindrical coordinates $r \sin\theta = y$ and $r \cos\theta = x$. The constant a_1 must be determined from boundary conditions. Using Eq. (9), the film profile is

$$h(x) \rightarrow \frac{D_v a_1}{\rho u_o} x^{1/2} \quad . \tag{14}$$

Fitting the data of Fig. 1 to the form $h=cx^{\nu}$ yields $\nu=0.50\pm0.01$, in agreement with Eq. (14), with $c^2\approx1$ Å. Taking $D_v\approx0.1$ cm^2/s and a saturation vapor pressure of about 40 torr (ethanol), we find $a_1\approx10^{-4}$ g cm$^{-7/2}$; the concentration drops by 10% at a distance of 1 cm from the film's surface.

Equation (14) holds over the experimentally observable range 50 μm < x < 1 cm, and it can be shown that the curvature is small in this range. Nearer the drying line, however, the capillary pressure cannot be ignored. Equation (8) can be improved by rescaling in view of Eq. (14). Let $\xi=\delta^{10}X$, $\phi=\delta^{10}\Phi$, and $j=\delta^{10}\Psi$, then ignoring higher powers in δ we obtain

$$\Phi^3 \Phi_{XXX} = 3(\Phi - \Psi) \quad , \tag{15}$$

which should be good when capillary pressure is important. Inevitably, the van der Waals forces will be dominant, since $\pi(\xi)\rightarrow\xi^{-n}$ (n=3 or 4), at which point static wetting should pertain [9].

The singularity strength (exponent) in Eq. (13) is sensitive to the geometry of the film. For coating a circular cylinder of decreasing radius, the strength passes from 1/2 for a large radius (because the film is locally a sheet) to 1 as the radius vanishes. This property can be demonstrated experimentally; we would expect a singularity of strength 1 for spinning sol-gel fibers.

SOL STRUCTURE AND CAPILLARY COLLAPSE

In the prototypical sol-gel process, silicates dissolved in alcohol are provided with varying amounts of water at a given pH to promote hydrolysis and subsequent condensation reactions. The polymers generated range from small, weakly branched, compliant oligomers to compact colloidal spheres depending on pH.

We can guess at the course of events during drying by following Scherer's analysis [10] for xerogels. After emerging from the drying line, the newly deposited film is still covered with liquid. As the liquid

evaporates and the gas-liquid interface begins to invade the pore space, menisci develop with a mean radius of curvature r that is initially infinite (flat) but rapidly decreasing. Assuming quasistatic conditions and good wetting (so that $\cos(\theta_{wet})$ is of order 1), there must be a pressure drop across the interface given by the Young-Laplace equation [11]

$$\Delta p = - \frac{2\gamma}{r} \quad , \tag{16}$$

where γ is the surface energy. The network will compress under the capillary pressure, eventually compacting beyond the elastic limit. In the last stages, the menisci have radii comparable to the pore size in the compacted network.

Now it is clear how the sol structure plays a role, since for non-interpenetrating clusters the size of the pores in the initial network will be comparable to the precursor size. Small precursors will normally have small pores with large capillary pressures, and vice versa for large particles. These trends have been observed [12] in the refractive index of films formed from silicate sols aged for as long as three weeks during which the precursor particles grew large enough to make the sol turbid. The refractive index, which is sensitive to the porosity, decreased from over 1.40 to below 1.20.

For a 1 μm pore half-filled with water, Eq. (16) implies a pressure difference of about 1 atm. Since the meniscus is curved away from the liquid, the pressure in the liquid is lower than that of the gas phase, and, for pores of 1 μm and smaller, the liquid pressure goes negative. One might expect the water simply to boil, limiting the pressure drop to about 1 atm. However, it appears that liquids in sufficiently small pores are able to overexpand, a condition analogous to superheating, because nucleation of vapor bubbles is suppressed by the small pore volume [13]. An estimate of the absolute limit of this overexpansion is given by the negative portion of the van der Waals loop, which represents metastable states with large chemical potential and is shown in Fig. 2 as the section from A to B. The maximum tensile pressure at B is of order 1000 atm, beyond which some part of the liquid spontaneously vaporizes.

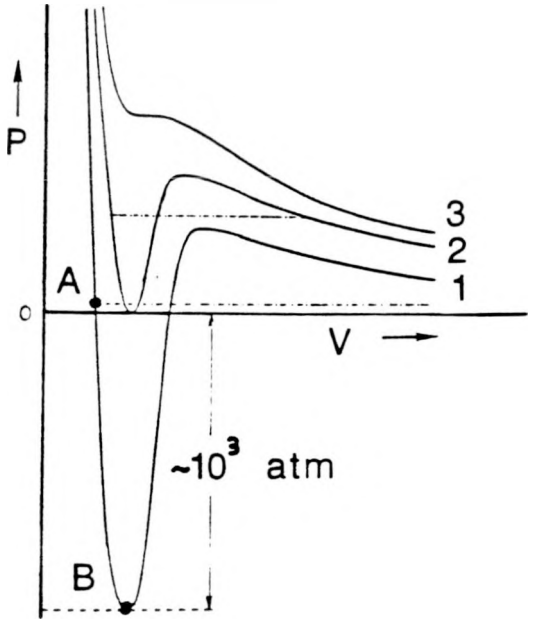

Figure 2. Van der Waals phase diagram for water. By the equal-area construction, point A represents equilibrium liquid. Overexpanded liquid in capillaries lie on the metastable branch AB. Higher temperatures are represented by lines 2 and 3. (From Ref. 13)

DISCUSSION

The determination of the entrained film profile provides a great deal of information about the environment experienced by a sol particle as it is carried from the reservoir to the drying line. By conservation of nonvolatile mass, the concentration of solids $\chi(x)$ must satisfy $\chi(x)h(x)$=constant for all positions above the "stagnation point"--the point on the liquid surface below which the liquid returns to the reservoir--which is normally in the gravitational meniscus region. Hence, for planar geometry we expect $\chi \sim x^{-1/2}$, i.e. the concentration diverges as the evaporation rate. The mean particle separation is quite precipitous, $\Delta r = \chi^{-1/3} \sim x^{1/6}$; half of the decrease in Δr occurs within the last 2% of the entrained film. The situation is not so clear for the rate of reaction, which can be characterized by the inverse of the time Δt for diffusing to the nearest particle. If the viscosity η diverges as χ^s, we have $\Delta t \sim \eta \Delta r^2 \sim x^{1/3-s/2}$; diffusion-limited reactions would be expected to accelerate if $s<2/3$.

With the possibility of pore liquid overexpansion, it is easy to see why capillary forces can be overwhelming during the capillary collapse stage of film formation. It is interesting that during this stage the pores are filled with the chemical equivalent (from a chemical potential standpoint) of superheated liquid [14], which may help to patch together any undone reactions (although transport is severely limited after deposition).

It should be possible to diminish the maximum tensile pressure by simply heating the liquid, as the upper curves in Fig. 2 illustrate. Thus, if the pore tensions are limited only by maximum overexpansion, heating during film formation would cause less capillary collapse.

There is an apparent difficulty with the argument regarding suppression of nucleation in small pores: the vapor phase is already present at the interface and shouldn't have to nucleate but simply to propagate--a dilemma not addressed in the literature. An alternative view, in which there would be less overexpansion, is that the the system adjusts its contact angle to keep the meniscus from curving beyond some value. The cost in free energy due to this accommodation at the contact line would be mitigated by less expansion work on the liquid.

It is important to note that, even if the menisci are flat (contact angle=90°) and the Laplace pressure drop is zero, strong forces and torques are exerted on the walls of the pore with the possibility of collapse. Detection of capillary pressures is an outstanding realm for experiments.

ACKNOWLEDGMENTS

The authors have benefited by helpful discussions with L. E. Scriven, P. R. Schunk and G. W. Scherer. This work was supported by Sandia National Laboratories under Department of Energy Contract DE-AC04-76-DP00789.

REFERENCES

1. H. Schroder, in Physics of Thin Films: Advances in Research and Development, edited by G. Haas and R. E. Thun, 5, 87 (1969).

2. C. J. Brinker, A. J. Hurd, G. C. Frye, K. J. Ward, and C. S. Ashley, in the Proceedings of the Fourth International Conference on Ultrastructure Processing of Ceramics, Glasses and Composites, J. Non-Crystalline Solids, (in press, 1990).

3. A. J. Hurd and C. J. Brinker, J. Phys. France 49, 1017 (1988).

4. L. Landau and B. Levich, Acta Physicochim. (URSS) 17, 42 (1942).

5. S. D. R. Wilson, J. Engg. Math. 16, 209 (1982).

6. A. J. Hurd and C. J. Brinker, in Better Ceramics Through Chemistry III, edited by C. J. Brinker, D. E. Clark, and D. R. Ulrich (Materials Research Society, Pittsburgh) 121, 731 (1988).

7. N. A. Fuchs, Evaporation and Droplet Growth in Gaseous Media, (Pergamon, London, 1959) chapter 1.

8. J. D. Jackson, Classical Electrodynamics, (Wiley, NY, 1975) section 2.11.

9. J. G. Truong and P. C. Wayner, Jr., J. Chem. Phys. 87, 4180 (1987).

10. G. W. Scherer, J. Non-Cryst. Solids 107, 135 (1989).

11. L. Landau and I. Lifshitz, Fluid Mechanics, (Pergamon, Oxford, 1959) chapter 7.

12. C. J. Brinker, A. J. Hurd, and K. J. Ward, in Ultrastructure Processing of Advanced Ceramics, edited by J. D. Mackenzie and D. R. Ulrich (Wiley, NY, 1988) p. 233.

13. C.G.V. Burgess and D. H. Everett, J. Colloid and Interface Sci. 33, 611 (1970).

14. L. E. Scriven, private communication (November, 1989).

DISCLAIMER